Demodulation of fiber Bragg grating sensor using cross-correlation algorithm

Author/Contributor:
Huang, C; Jing, W; Liu, K; Zhang, Y; Peng, Gang-Ding

Publication details:
IEEE Photonics Technology Letters
v. 19
Chapter No. 9-12
pp. 707-709
1041-1135 (ISSN)

Publication Date:
2007

Publisher DOI:
http://dx.doi.org/10.1109/LPT.2007.895422

Demodulation of Fiber Bragg Grating Sensor Using Cross-Correlation Algorithm

Cen Huang, Wencai Jing, Kun Liu, Yimo Zhang, and Gang-Ding Peng

***Abstract*—In this letter, a demodulation algorithm for fiber Bragg grating (FBG) sensor is presented. The proposed demodulation algorithm evaluates the wavelength shift in the reflected spectrum of an FBG sensor. It computes the cross-correlation between the perturbed spectrum and the undisturbed spectrum. We compare the proposed algorithm with another three reported algorithms and then discuss the experimental results in respect of the reflective index of FBGs and other factors that may influence the sensing resolution. We report strain resolutions of 0.4 and 1.5 $\mu\varepsilon$ in high reflective gratings and low reflective gratings, respectively.**

***Index Terms*—Cross-correlation, demodulation algorithm, fiber Bragg grating (FBG), strain sensor.**

I. Introduction

FIBER Bragg gratings (FBGs) have been widely adopted in measuring of statistic and dynamic parameters such as temperature, strain, and stress [1]. With mixed wavelength-division-multiplexing and time-division-multiplexing techniques, a series of sensor gratings can be interrogated along a single optical fiber for distributed sensing. While various FBG demodulation schemes based on a tunable laser source [2] or a broadband source in conjunction with a wavelength-selective component [3] have been developed, the primary task invariably comes to the demodulation algorithm for precise determination of the often slight measurand induced wavelength shift from the reflected or transmitted spectrum. However, the direct peak detection method always produces poor results, especially in the system with a low signal-to-noise ratio (SNR). In previous works [4]–[6], many demodulation algorithms have been proposed, such as centroid detection algorithm (CDA) [4], least squares algorithm (LSQ) [5], and the autocorrelation algorithm [6]. Here we present and demonstrate an accurate demodulation algorithm based on cross-correlation. The wavelength shift is calculated by cross-correlation product between the undisturbed spectrum and the perturbed spectrum of an FBG. In Section III, we demonstrate the characteristics of the proposed algorithm with a devised experiment. Meanwhile, it is compared with another two demodulation algorithms. The demonstrated configuration is established based on Virtual Instrument technology for controlling the tunable laser source and power meter as well as processing experimental data. All the algorithms are realized with Labview programs.

Manuscript received January 3, 2007; revised March 1, 2007.

C. Huang, K. Liu, and Y. Zhang are with the College of Precision Instrument and Opto-Electronics Engineering, Tianjin University, Tianjin 300072, China, and also with the Key Laboratory of Opto-Electronics Information and Technical Science (Tianjin University), Ministry of Education, Tianjin 300072, China.

W. Jing is with the College of Precision Instrument and Opto-Electronics Engineering, Tianjin University, Tianjin 300072, China, also with the Key Laboratory of Opto-Electronics Information and Technical Science (Tianjin University), Ministry of Education, Tianjin 300072, China, and also with the School of Electrical Engineering and Telecommunications, University of New South Wales, Sydney NSW 2052, Australia.

G.-D. Peng is with the School of Electrical Engineering and Telecommunications, University of New South Wales, Sydney NSW 2052, Australia.

Digital Object Identifier 10.1109/LPT.2007.895422

II. Demodulation Algorithm Principle

The basic principle of the operation used in an FBG sensor is the monitoring of the wavelength shift of the reflected spectrum in response to a change in the measurand. In the proposed demodulation algorithm, an undisturbed reflected spectrum is obtained first. This spectrum is recorded as an array with N samplings length $R(\lambda_i)$ for $i = 0, 1, 2, \ldots, (N-1)$. The number of samplings is determined by the following equation:

$$N = \frac{\lambda_{\max} - \lambda_{\min}}{\delta\lambda} \tag{1}$$

where $\lambda_{\max} - \lambda_{\min}$ is the scanning range of the tunable laser and $\delta\lambda$ is the wavelength step of it. When the measurands, such as strain and stress are imposed on the grating, a perturbed reflected spectrum is recorded as $R'(\lambda_i)$, for $i = 0, 1, 2, \ldots, (N-1)$. Given the premise that the shape of perturbed reflected spectrum remains constant under the influence of measurands, which is widely accepted, the perturbed reflected spectrum becomes [6]

$$R'(\lambda_i) = R(\lambda_i - \Delta\lambda) \tag{2}$$

where $\Delta\lambda$ is the wavelength shift between the undisturbed and the perturbed reflected spectrum. In the proposed demodulation algorithm, the wavelength shift $\Delta\lambda$ is calculated from the cross-correlation product C_j by implementing the following equation:

$$C_j = \sum_{i=0}^{N-1} R(\lambda_i) R'(\lambda_{j+1-N-1}) \tag{3}$$

for $j = 0, 1, 2, \ldots, 2N-2$ and C_j is an output sequence containing $2N-1$ samplings. This equation assumes that the indexed elements of $R(\lambda_i)$ and $R'(\lambda_i)$ that lies outside their ranges are equal to zero. This assumption is acceptable as long as the sampling number N is large enough so that the scanning range can cover the whole principal power peak in the reflected spectrum. In addition, the sequence C_j actually represents the correlation values when the reflected spectrum shifts $2N-1$ times in indexing. Given the (2) and (3), the values of the cross-correlation product C_j are distributed in accordance with a Gaussian profile. The wavelength shift $\Delta\lambda$ and the central wavelength of perturbed spectrum λ'_B can be calculated by the following equations:

$$\Delta\lambda = (p - N)\delta\lambda \tag{4}$$

$$\lambda'_B = \lambda_B + \Delta\lambda \tag{5}$$

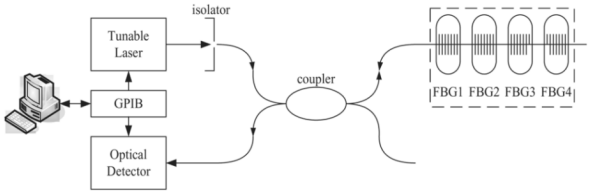

Fig. 1. Experimental configuration.

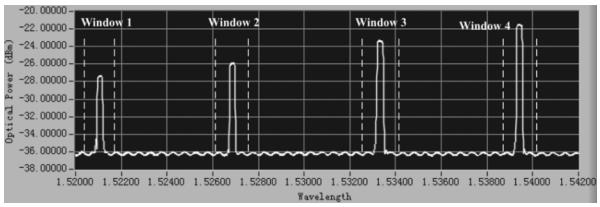

Fig. 2. Reflected spectrum. The four windows are 1600 pm wide.

where P is the x-coordinate of the center peak in Gaussian profile and λ_B is the central wavelength of undisturbed spectrum. In practical application, extra sampling points may be acquired and the N is determined by the number of sampling points that are actually involved in the correlation calculation. The resolution on the determination of $\Delta\lambda$ is closely linked to $\delta\lambda$ and thus, to the measurement device. A higher resolution can be obtained by implementing a Gaussian peak fitting on the correlation output sequence.

III. Experiments and Results

In this section, we demonstrate the resolution of the proposed algorithm as well as those of another three algorithms. The experimental setup is shown in Fig. 1.

In the configuration, the light is emitted from HP 81640 A tunable laser controlled by computer via GPIB bus. The reflected light from FBGs via 3-dB coupler is detected by the optical detector, HP 81531 A power meter, which transmits the data of reflected spectra to computer for synchronous processing and display. The four FBGs are incorporated upon a single fiber and marked with FBG1, FBG2, FBG3, and FBG4, respectively. No intended strain is imposed on any of the gratings. The FBG4 with the highest reflected power performs as a reference grating to compensate the fluctuation of ambient temperature. As the scanning wavelength increases from 1520 to 1542 nm with a 5-pm step, a reflected spectrum with 4400 sampling points is recorded, approximately 1100 sampling points for each FBG. With the given scanning wavelength step, windows are set to determine the N in (1), number of sampling points involved in the correlation calculation. The reflected spectrum with four windows is displayed in Fig. 2.

This procedure is repeated for 10 000 times and the computed strains will vary according to a normal distribution theoretically. By observing the standard deviation of strains on the gratings, we demonstrate the resolution of the proposed algorithm as well as other algorithms. The reflected spectrum obtained in the first scanning route is recorded as the undisturbed spectrum, namely the reference spectrum. Another Labview program is designed to compute the strain undulation on the other three gratings by calculating the cross-correlation products between the reference spectrum and each of the other 9999 reflected spectra. The data is processed with four algorithms and the width of the wavelength windows are set to 1600 pm ($N = 320$). The computed standard deviations of strain on the FBGs are presented in Table I.

TABLE I
Computed Resolutions of the Algorithms

Standard Deviation ($\mu\varepsilon$)	FBG1	FBG2	FBG3
Cross-Correlation	1.5	1.2	0.4
CDA	2.0	1.5	0.5
LSQ	3.0	1.6	0.5
Autocorrelation	5.9	5.7	1.1

The proposed demodulation algorithm results in the highest resolutions of 1.5 and 0.4 $\mu\varepsilon$ on FBG1 and FBG3, respectively. In other words, compared with the CDA, LSQ, and the autocorrelation algorithm, the proposed algorithm improves the resolution by 20%, 20%, and 74% in FBG3 and 25%, 50%, and 78% in FBG1, respectively.

Particularly, the strain sensitivity of FBG3 is 1.2 pm/$\mu\varepsilon$. We thus achieve a resolution of 1.3 pm in FBG3 by using the autocorrelation algorithm. This result keeps in accordance with [6], where a resolution of 1 pm is reported, using the autocorrelation algorithm. However, the same algorithm produces rather poor results when applied on the FBG1 and FBG2. Actually, in the autocorrelation algorithm, a few hundreds of vectors composed of N samples are obtained after the calculation of the autocorrelation product between the reference spectrum and the shifted spectrum. Only the samples with the maximum amplitude of each vector are selected and involved in the final determination of the wavelength shift [6]. However, such direct detection of the samples with maximum amplitude could be rather inaccurate due to the system noise, quantization error during data acquisition or imperfection of gratings, to name a few. The proposed algorithm eliminates this disadvantage by including all the computed samples of every vector into the final determination of wavelength shift. And compared with the autocorrelation algorithm, it improves the resolution by more than 60% in all the three FBGs, according to Table I. The computing time does not increase significantly because the extra calculation is just floating add instead of multiplication. The time for every correlation calculation is about 10 ms on a computer with a Pentium 2.8-GHz dual-core CPU and 512M RAM. Therefore, the proposed algorithm allows a 100-Hz scanning frequency which can meet the requirements of most dynamic sensing systems.

To further improve the resolution of the system, an iterative loop is developed in the designed Labview program. It enables the windows in Fig. 2 to move automatically with the reflected spectra's small shift due to slight ambient temperature undulation. The relation between the resolution and the width of wavelength windows under a given step size of 5 pm is presented in Fig. 3

Steady evolutions of the resolutions are observed as the width of wavelength windows is set within the range from 300 to 1600 pm, that is 60 to 320 for N, the sampling points number. The resolutions begin to deteriorate when the width of wavelength windows approaches 200 pm, the 3-dB bandwidth of FBGs. However, rapid descents appear when 100-pm-wide windows and 150-pm-wide windows are applied. These values are

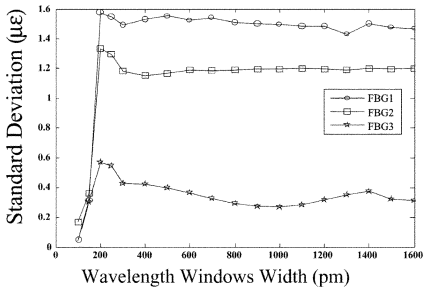

Fig. 3. Evolution of resolutions versus wavelength windows width. The 3-dB bandwidths of the three FBGs are approximately 200 pm.

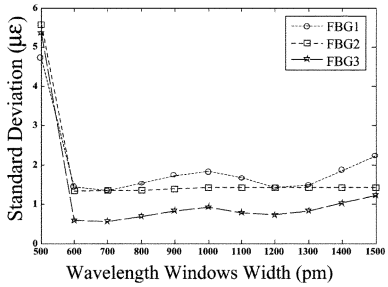

Fig. 4. Evolution of resolutions versus wavelength windows width (CDA).

unconvincing for the reason that the width of windows is smaller than the 3-dB bandwidth of FBGs. And the information of the raising and falling edges of the principal peaks in the reflected spectrum is lost. The evolution of resolutions with respect to wavelength windows width using CDA is presented in Fig. 4.

By comparing Fig. 3 with Fig. 4, we find that the proposed algorithm desires a narrower window to assure a high resolution than the CDA does. This can not only reduce the computing time but, more importantly, it can reduce the number of sampling points with low reflected power, which often limit the resolution of many other algorithms. Table I renders support to this point. In Table I, the resolutions of each algorithm yield to the reflective index of the gratings in that the highest resolution of each algorithm invariably lies in the FBG3 with the highest reflected power, which can lead to the highest SNR (13.5 dB). In this experiment, the SNR for FBG2 is 11 dB. It is about 60% more than the SNR for FBG1. The resolution of the cross-correlation algorithm on FBG1 almost equals to those of CDA and LSQ on FBG2 and is much better than that of autocorrelation on FBG2. It means that the proposed algorithm can guarantee a satisfying resolution even in the demodulation system with a lower SNR. This can lower the requirements on the system and reduce the system cost consequently. In the [6], [7], twin Bragg gratings are used to solve this problem so that the autocorrelation algorithm could be applied in the demodulation system with low reflective gratings. And the reported result is satisfying. However, this method desires two identical Bragg gratings and their Bragg wavelengths must be exactly the same. Writing such gratings is more difficult and expensive than writing a single grating.

We increase the scanning wavelength step of the tunable laser from 5 to 100 pm by an interval of 5 pm and repeat the resolution experiment mentioned above. Fig. 5 displays the evolution of resolution with respect to wavelength step. When the scanning wavelength step is restricted under 40 pm, the standard deviations of all the three FBGs evolve steadily. However, when it exceeds 40 pm, the standard deviations vary in a large scale. This behavior is predictable because of the concomitant increasing extrapolation error of Gaussian peak fitting. Therefore, a scanning wavelength step of 40 pm which can be realized by most tunable lasers can guarantee a high sensing resolution. This can reduce the system cost further more. The sensing resolution can be further improved by using a tunable laser source allowing wavelength steps as short as 1 pm or replacing the single FBGs with twin FBGs.

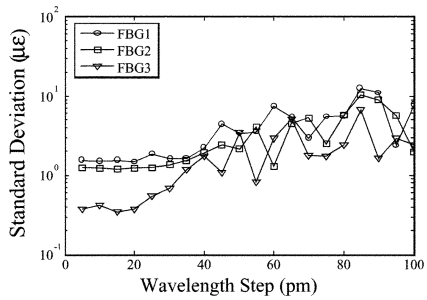

Fig. 5. Evolution of resolutions versus wavelength step. The width of the wavelength windows is fixed at 1600 pm.

IV. Conclusion

We have presented a demodulation algorithm based on Virtual Instrument technology. Besides the demonstrated configuration, this algorithm can be applied in many other FBG demodulation schemes. Due to its fast demodulation speed, the proposed algorithm can be implemented in the demodulation schemes for dynamic sensing and measurements of temperature or strain. And this algorithm can be easily transplanted into an embedded FBG sensing system. The devised experiment shows that the proposed algorithm results in the highest resolutions among the four algorithms. Moreover, in the presence of low reflected power of FBG sensors, the proposed algorithm produces significantly better results than those of other algorithms. This makes the proposed algorithm perform well even in a low SNR system or with a long scanning wavelength step and thus can save the system cost to a large extent.

References

[1] A. D. Kersey, M. A. Davis, H. J. Patrick, M. LeBlanc, K. P. Koo, C. G. Askins, M. A. Putnam, and E. J. Friebele, "Fiber grating sensors," *J. Lightw. Technol.*, vol. 15, no. 8, pp. 1442–1442, Aug. 1997.

[2] G. A. Ball, W. W. Morey, and P. K. Cheo, "Fiber laser source/analyzer for Bragg grating sensor array interrogation," *J. Lightw. Technol.*, vol. 12, no. 4, pp. 700–703, Apr. 1994.

[3] A. D. Kersey, T. A. Berkoff, and W. W. Morey, "Multiplexed fiber Bragg grating strain-sensor with a fiber Fabry–Pérot wavelength filter," *Opt. Lett.*, vol. 18, pp. 1370–1372, 1993.

[4] C. G. Atkins, M. A. Putnam, and E. J. Friebele, "Instrumentation for interrogating many-element fiber Bragg grating arrays," *Proc. SPIE*, vol. 2444, pp. 257–257, 1995.

[5] A. Ezbiri, S. E. Kanellopoulos, and V. A. Handerek, "High resolution instrumentation system for fibre-Bragg grating aerospace sensors," *Opt. Commun.*, vol. 150, pp. 43–48, 1998.

[6] C. Caucheteur, K. Chah, F. Lhommé, M. Blondel, and P. Mégret, "Autocorrelation demodulation technique for fiber Bragg grating sensor," *IEEE Photon. Technol. Lett.*, vol. 16, no. 10, pp. 2320–2322, Oct. 2004.

[7] ——, "Characterization of twin Bragg gratings for sensor application," *SPIE Proc. Photonics Europe*, vol. 5459, pp. 89–100, 2004.